The inactivation of GPx4 by ferroptosis-inducing molecule RSL3 requires an adaptor protein: evidence for 14-3-3ε

Ana-Marija Vučković, Valentina Bosello Travain, Luciana Bordin, Giorgio Cozza, Giovanni Miotto, Monica Rossetto, Stefano Toppo, Rina Venerando, Mattia Zaccarin, Matilde Maiorino, Fulvio Ursini and Antonella Roveri*

Department of Molecular Medicine, University of Padova, 35121-Padova, Italy

*corresponding author:
Antonella Roveri, Department of Molecular Medicine, University of Padova, Viale G. Colombo, 3, I-35131-Padova, Italy;
antonella.roveri@unipd.it tel. (+39) 049-8276102; fax. (+39) 049-8073310

ABSTRACT

RSL3, a drug candidate prototype for cancer chemotherapy, triggers ferroptosis by inactivating GPx4. Here we report the purification of the protein indispensable for GPx4 inactivation by RSL3. MS analysis reveals 14-3-3 isoforms as candidates and recombinant human 14-3-3ε confirms the identification. The function of 14-3-3ε is redox-regulated. Moreover, overexpression and silencing of the gene coding for 14-3-3ε consistently control the inactivation of GPx4 by RSL3. The interaction of GPx4 with a redox-regulated adaptor protein, operating in cell signalling, further contributes to frame it within redox-regulated pathways of cell survival and death and opens new therapeutic perspectives.

Keywords: RSL3, ferroptosis, glutathione peroxidase 4, 14-3-3 proteins, protein-protein interaction, redox regulation.

Abbreviations: RSL3, Ras-selective lethal small molecule 3; GPx4, glutathione peroxidase 4; PC-OOH, phosphatidylcholine hydroperoxide; MS, mass spectrometry; GSH, glutathione; DMSO, dimethyl sulfoxide; CHAPS, 3-(3-cholamidopropyl) diethyl-ammonio-1-propanesulfonate; ACN, acetonitrile; TCEP, Tris(2-carboxyethyl)phosphine hydrochloride.

INTRODUCTION

Glutathione Peroxidase 4 (GPx4, EC 1.11.1.12). is a deeply characterized selenoprotein belonging to the family of glutathione peroxidases. It reduces membrane lipid hydroperoxides to corresponding alcohols using glutathione (GSH) as reducing substrate, hence originally named Phospholipid Hydroperoxide Glutathione Peroxidase (1). Like many other mammalian glutathione peroxidases, GPx4 harbors a selenocysteine as redox-active moiety allowing a fast rate of lipid hydroperoxide reduction. Since membrane lipid peroxidation requires a continuous production of lipid radicals from ferrous iron-mediated decomposition of lipid hydroperoxides, GPx4 holds unique lipid peroxidation inhibiting attributes (2).

The compound (1*S*,3*R*)-RSL3 was developed by Stockwell et al. seeking for an anti-cancer drug candidate. (1*S*,3*R*)-RSL3 was identified in a synthetic lethal screening aimed to identify small molecules inducing death on cells bearing oncogenic RAS (3). It was found that, in sensitive cells, (1*S*,3*R*)-RSL3 induces a non-apoptotic form of cell death, which is prevented by either antioxidants or iron chelation. Since the cellular labile iron pool emerged indispensable for the lethal effect, this new form of death was named ferroptosis (3-6).

Ferroptosis is also induced by inhibiting the cystine-glutamate antiporter system (x_c^-) by the compound erastin (7-8). In this model, erastin primes ferroptosis by dampening cystine uptake, which is the indispensable source of cysteine for GSH biosynthesis (8). It became soon evident that the death phenotype of ferroptosis fully overlapped with that primed by GPx4 whole gene deletion in mouse or cell models. The shared mechanism of these cell death phenotypes is the missing inhibition of membrane lipid peroxidation (9-14). Consistently, an unbiased, affinity-based chemo proteomic approach identified GPx4 as the target of (1*S*,3*R*)-RSL3. Notably, the (1*R*,3*R*)-RSL3 diastereomer did not exhibit lethality in sensitive cells, probing the specificity of the interaction (11). The notion that GPx4 is the target of (1*S*,3*R*)-RSL3 was further validated by genetic manipulation of cells, demonstrating sensitization or resistance to (1*S*,3*R*)-RSL3 when GPx4 was partially knocked-out or overexpressed, respectively (11).

Besides a suitable target for cancer chemotherapy (15), ferroptosis is seen today as the widespread mechanism of regulated cell death underlying neurodegeneration, ischemia-reflow, kidney failure, metabolic syndrome and septic shock (16). Since the pharmacological, and, seemingly, pathophysiological inhibition of GPx4 is the core of ferroptosis, the elucidation of the details of the inactivation by

(1*S*,3*R*)-RSL3 attracted our attention also in the view of a possible general mechanism in which (1*S*,3*R*)-RSL3 could mimic the action of electrophiles generated under physiological conditions.

In this paper, we provide evidence that (1*S*,3*R*)-RSL3 does not inactivate purified GPx4 while it is fully efficient in the presence of a redox sensitive cytosolic factor. Adopting a typical biochemical chromatographic approach and mass spectrometry we identified 14-3-3 proteins necessary for this function. This identification was functionally validated using recombinant human 14-3-3ε.

For sake of simplicity, in the text we refer to the active form (1*S*,3*R*)-RSL3 as RSL3, when not specifically needed.

MATERIALS AND METHODS

Reagents and cells

GPx4 was purified from rat testis cytosol through four chromatographic steps performed in sequence: glutathione-bromosulfophthalein affinity chromatography, hydrophobic interaction chromatography, ion exchange chromatography and size exclusion chromatography, according to the protocols detailed in (17).

Protein concentration was 0.05 mg mL^{-1} and specific activity was 130 μmol $mg^{-1}min^{-1}$ at 25°C in the presence of 2.5 mM GSH and 30 μM phosphatidylcholine hydroperoxide (PC-OOH). Activity was measured in 1 mL coupled test with Glutathione Reductase (EC 1.8.1.7) as described in (18). Further details for GPx4 purification and activity test are reported under Supporting information. RSL3 (99.76% purity, Selleckchem, U.S.A) and (1*R*,3*R*)-RSL3 (generous gift of Drs W.S. Yang and B.R. Stockwell) were kept at -20°C as 30 mM stock solutions in DMSO. HEK293T cells (ATCC® CRL-3216™, generous gift of Prof. S. Piccolo, University of Padova) were cultured in DMEM, high glucose, GlutaMAX™ supplement (Gibco, Thermo Fisher Scientific Inc., U.S.A) containing 10% (v/v) FBS, 1% (v/v) penicillin/streptomycin.

Preparation of cytosol

HEK293T cell cytosol was prepared in homogenizing buffer (HB), i.e. 100 mM Tris-HCl, 250 mM sucrose, pH 7.4, containing a cocktail of protease inhibitors, by 100 strokes of a hand-held, low clearance, glass homogenizer (Kontes, U.S.A). HEK293T cells from a 75 cm^2 flask, at about 70% confluency, were homogenized in 0.3 mL of buffer. The homogenate was centrifuged at 105,000x*g* for one hour and the supernatant used for experiments.

Organ cytosols were from adult Sprague–Dawley male rats. All experimental procedures were performed according to institutional guidelines in compliance with national (D.L. 116/1992) and international law and policies (European Council directive 86/609/EU and new directive 2010/63/EU; US National Research Council, Guide for the Care and Use of Laboratory Animals, 8th edition, 2011). One gram of tissue was homogenized in 3 mL of HB by a Potter-Elvehjem glass-teflon homogenizer. Cytosols were the final supernatants obtained through differential centrifugation at 500x*g* for 5 minutes, 9,000x*g* for 20 minutes and 105,000x*g* for one hour.

Measurement of the activity permitting GPx4 inactivation by RSL3

Purified GPx4 was treated with 30 mM 2-mercaptoethanol for one hour in an ice-cold bath and thoroughly freed from thiol just before the experiment by buffer exchange on PD SpinTrap™ G-25 (GE Healthcare, Sweden) equilibrated with 50 mM KH_2PO_4/K_2HPO_4, 1 mM EDTA, 0.05% CHAPS (w/v), pH 7.0. GPx4 was then used within three hours. For an inactivation test, cytosol (0.05 mg protein for cells and 0.15 mg protein for organs) and GPx4 (100 ng) were diluted in 0.1 mL of HB. Each sample was split into two identical volumes and 0.1 mM RSL3 diastereomer (treated), or an equal volume of solvent (blank) were added. For rat organs the amount of purified rat GPx4 added was indeed slightly variable in order to compensate for the activity endogenously present in samples. Controls were carried out by diluting GPx4 in HB. After 20 minutes' incubation at 25°C, GPx4 activity was measured and the results were expressed as the percentage of residual GPx4 activity in RSL3-treated samples *vs* the corresponding blanks.

For a quantitative evaluation of the inactivation-permitting activity, its units (U) were defined as follows. One U is the amount of inactivation-permitting activity yielding 50% GPx4 inactivation under definite conditions: inactivation test volume: 0.05 mL, added GPx4 (50 ng, specific activity: 130 μmoles $mg^{-1}min^{-1}$), RSL3 concentration (0.1 mM), time of incubation (twenty minutes) and temperature (25°C).

In some experiments HEK293T cytosol was treated with 10 mM diamide for thirty minutes in an ice-cold bath and freed from the thiol-oxidizing agent by buffer exchange on PD SpinTrap™ G-25 equilibrated with HB containing 0.05% CHAPS (w/v). It was then used in the inactivation test either with or without 2.5 mM Tris(2-carboxyethyl)phosphine hydrochloride (TCEP).

Purification of the inactivation-permitting protein(s)

Wide-range molecular weight separations of components of rat kidney cytosol were obtained through centrifugal concentration at different cut off of molecular weight using Vivaspin® 500 MWCO 50000 and Vivaspin® 500 MWCO 100000 (Sartorius, Germany).

Purification of the inactivation-permitting activity was achieved by three chromatographic steps: hydrophobic interaction chromatography on phenyl-sepharose® CL-4B (GE Healthcare, Sweden), ion exchange chromatography on a MonoQ column (Resource™ Q, 6 mL, GE Healthcare, Sweden) and size exclusion chromatography on Superdex™ 75 10/300 GL (GE Healthcare, Sweden). All the purification steps were performed at 4°C in a ÄKTA™ pure 25 chromatographic system (GE Healthcare, Sweden).

All chromatographic fractions to be tested for the inactivation-permitting activity were in 50 mM KH_2PO_4/K_2HPO_4, 1 mM EDTA, 2.5 mM GSH, 0.05% CHAPS (w/v), pH 7.0. When necessary, concentration by a DiaFlo apparatus equipped with a YM-10 ultrafiltration membrane (Millipore, USA) and a buffer exchange in Illustra NAP™-5 columns (GE Healthcare, UK) were carried out. Purified GPx4 (100 ng) was added to a 0.1 mL aliquot of each fraction, and equal volumes were then incubated either with 0.1 mM RSL3 (treated) or the same volume of solvent (blank), for 20 minutes at 25°C. After incubation, GPx4 activity was measured and the corresponding units of inactivation-permitting activity were calculated. Details of the purification steps are available in Supporting information.

MS analysis of the fractions from size-exclusion chromatography

Positive fractions from the last purification step were used to identify the protein(s). Samples were thoroughly dialyzed against water and brought to dryness in a Savant SpeedVac® SVC-100 concentrator (SVPT S.r.l., Italy). Protein pellets were digested in 0.1 mL of 40 mM NH_4HCO_3, 10% (v/v) acetonitrile (ACN) containing 10 ng of Trypsin (Trypsin Gold Mass Spectrometry Grade, Promega Co, U.S.A). Digestion was carried out at 37°C overnight and stopped by adding formic acid to lower the pH to 3 – 4. Samples were dried and dissolved in 20 μl of 5% (v/v) ACN, 0.1% (v/v) formic acid aqueous solution.

Tryptic peptides were analyzed on a 1200 nano-HPLC system coupled to a 6520 Accurate-Mass Q-TOF equipped with a HPLC-Chip cube interface as nano-ESI (Agilent Technologies, U.S.A.). Data were acquired with Mass Hunter Data Acquisition software, ver.B.05.00 (Agilent Technologies, U.S.A.) in positive ion mode, in the range between 59 and 1700 m/z, at a MS and MS/MS scan rate of 3

Hz with a resolving power of 20,000 FWHM. MS/MS precursors were selected in data-dependent mode on the five most intense precursors from each scan at an isolation width of 4 a.m.u. and fragmented by collision-induced dissociation by the application of a formula weighting collision energy based on precursor charge and m/z. Raw data of MS/MS datasets were searched with Mascot search engine with an in-house server version of Mascot rev. 2.3 (Matrix Science) against the whole SwissProt database with no taxonomy restriction. Search constraints were: 10 p.p.m. tolerance for precursor ion masses and 0.05 Da tolerance for fragment ion masses. Trypsin enzyme restriction specificity was imposed for peptides, with a maximum of two missing cleavages. Further details are reported in Supporting information.

Production and purification of recombinant human 14-3-3ε

Cloning of the open reading frame of human14-3-3ε (access n. NM_006761.5) with the N-terminal GST tag was done in the vector pGEX-6P-1, using the cloning site BamHI-XhoI, and was provided by GenScript (Hong Kong, HK). The cloned 14.3.3ε sequence is reported in Supporting information. The correctness of the construct was verified by sequencing.

To produce human recombinant protein, competent BL21 pLysS *E. Coli* cells were transformed with the human 14-3-3ε_pGEX-6P-1 expression vector. The expression was induced by adding 1 mM isopropyl-β-D-thiogalactopyranoside (Promega Co, U.S.A) to the culture broth at 37°C for 4 hours. Eventually, cells from 0.2 L broth were harvested by centrifugation at 5,000xg for 30 min at 4ºC.

The bacterial pellet was extracted by 20 mL B-PER® bacterial protein extraction reagent (Pierce, Rockford, U.S.A), containing a mixture of protease inhibitors, under continuous stirring, for 20 min on an ice-cold bath. The extraction mixture was then centrifuged at 35,000xg for 30 min and the supernatant diluted 1 to 10 (v/v) with 10 mM Na_2HPO_4, 1.8 mM KH_2PO_4, 140 mM NaCl, 2.7 mM KCl, pH 7.3 before loading onto a GSTrap™ FF 1 mL column (GE Healthcare, Sweden). GST-tag was removed by PreScission Protease (GE Healthcare, Sweden) cleavage, according to the manufacturer's instructions. Recombinant human 14-3-3ε was further purified by hydrophobic interaction and size exclusion chromatography, previously reported.

GPx4 inactivation-permitting activity of 14-3-3ε

In all the inactivation experiments recombinant 14-3-3ε and GPx4 were previously treated with 2.5 mM GSH and 30 mM 2-mercaptoethanol, in an ice-cold bath for one hour, freed from thiol by buffer exchange on PD SpinTrap™ G-25 equilibrated with 50 mM KH_2PO_4/K_2HPO_4, 1 mM EDTA, 0.05% (w/v) CHAPS, pH 7.0. They were used within 2-3 hours, otherwise 2.5 mM GSH or TCEP were present during the inactivation experiment. In a standard 0.1 mL inactivation test GPx4 and 14-3-3ε concentrations were 40-50 nM and 0.25-0.5 μM, respectively. The inactivation test was carried out as described for cytosol.

Recombinant 14-3-3ε in 50 mM KH_2PO_4/K_2HPO_4, 1 mM EDTA, 0.05% (w/v) CHAPS, pH 7.0 was treated with 10 mM diamide for thirty minutes in an ice-cold bath and freed from the thiol-oxidizing agent by buffer exchange before the inactivation experiment. Briefly, GPx4 (50 nM) and diamide-treated 14-3-3ε (0.5 μM) were mixed, the resulting volume was split into two and treated with either 0.1 M RSL3 or solvent. The same experiment was also performed in the presence of 2.5 mM TCEP.

Increasing concentrations (0.25 μM to 1.9 μM) of purified recombinant 14-3-3ε in 0.25 mL of 50 mM KH_2PO_4/K_2HPO_4, 1 mM EDTA, 2.5 mM GSH, 0.05% (w/v) CHAPS, pH 7.0, were mixed with GPx4 (50 nM). Aliquots (0.05 mL) of each mixture were incubated with different RSL3 concentrations, 0.1 μM to 10 μM, for 20 minutes at 25°C. An aliquot was incubated with solvent for blank. For each concentration of 14-3-3ε the percentage of residual GPx4 activity with different RSL3 concentrations was calculated on the basis of the corresponding blank. In controls 14-3-3ε buffer substitutes for the protein.

MS analysis of GPx4 upon incubation with RSL3 and 14-3-3ε

To search for the product of interaction between GPx4 and RSL3, reduced recombinant 14-3-3ε (0.02 mg) and rat GPx4 (0.01 mg) in 50 mM KH_2PO_4/K_2HPO_4, 1 mM EDTA, 2.5 mM GSH, 0.05% (w/v) CHAPS, pH 7.0, were incubated with 0.1 mM RSL3 for twenty minutes at 25°C. After incubation, proteins were carboxymethylated (19) and further treated as described for chromatographic fractions before MS analysis.

MS/MS datasets were searched against ad hoc-built database for GPx4; considered variable modifications were: a) carboxymethylation on cysteine/selenocysteine, b) de-amidation on arginine/glutamine, c) RSL3 on

cysteine/selenocysteine/methionine, d) dehydroalanine from selenocysteine/selenenylamide.

Kinetic constants measurement

Recombinant 14-3-3ε (0.2 μM) and GPx4 (50 nM) or GPx4 alone were diluted in 0.2 mL of 50 mM KH_2PO_4/K_2HPO_4, 1 mM EDTA, 0.05% (w/v) CHAPS, pH 7.0 containing three different GSH concentrations (2, 3, 4 mM) and incubated in an ice-cold bath for one hour before kinetics experiments. Aliquots (0.05 mL) of each mixture were tested with the same concentrations of GSH in the activity test (18). Briefly: reactions were carried out at 25°C in 0.1 M KH_2PO_4/K_2HPO_4 pH 7.8 containing 5 mM EDTA, 0.1% (v/v) Triton X-100, 0.16 mM NADPH and 180 IU mL^{-1} Glutathione Reductase and different GSH concentrations (2, 3, 4 mM). The oxidant substrate, (45 μM) PC-OOH, triggered the enzymatic reaction. In the activity test GPx4 concentration was 2.5 nM and, when present, 14-3-3ε concentration was 10 nM.

Second order rate constants of the peroxidatic and reductive steps of GPx4 reaction were measured essentially according to (18).

Absorbance data at 340 nm were collected from progression curves of NADPH oxidation by a Varian Cary® 50 Scan UV/Vis spectrophotometer (Agilent Technologies, U.S.A). A 6.22 $M^{-1}cm^{-1}$ extinction coefficient was used for calculations. Kinetic analysis was carried out from single progression curves of NADPH oxidation at different GSH concentrations; absorbance data *vs* time were used to calculate substrate concentration and rate at time intervals of 5 seconds. Apparent rate constants for GPx4 alone and in the presence of 14-3-3ε protein were calculated by the simplified Dalziel equation (20):

$E/v_0 = \phi_0 + \phi_1/[\text{PC-OOH}] + \phi_2/[\text{GSH}]$, where: ϕ_0 is the reciprocal of the turnover number, which approximates to 0 (21) for GPx4 as for the other GPxs; ϕ_1 and ϕ_2 are the Dalziel coefficients, equivalent to the reciprocal of the second order rate constant of the oxidative and cumulative reductive steps of the reaction, respectively.

Protein-protein interaction assay

Reduced recombinant 14-3-3ε (12.5 μM) and GPx4 (3.5 μM) in 50 mM KH_2PO_4/K_2HPO_4, 50 mM KCl, and 0.05% (w/v) CHAPS, pH 7.0, were incubated in the presence of EZ-link™ NHS-PEG_4-Biotin (Thermo Fisher Scientific Inc., U.S.A) at 1:20 molar ratio, for one hour in an ice-cold bath. Free biotin was removed by

thorough buffer exchange in the same buffer and biotinylated 14-3-3ε and biotinylated GPx4 were concentrated to 0.12 mg mL^{-1} and 0.06 mg ml^{-1}, respectively.

Biotinylated 14-3-3ε and GPx4 (1.5 μg and 100 ng, respectively) in 0.1 mL were incubated with 0.2 mM RSL3 or solvent in the presence of 2.5 mM GSH, for 20 minutes at 25°C. Under these experimental conditions GPx4 was completely inactivated. Samples were affinity purified by reacting with 0.03 mL of streptavidin magnetic beads, 10 mg mL^{-1} (Thermo Fisher Scientific Inc., U.S.A.) for 2-3 minutes; beads were then quickly washed three times with 0.1 mL of incubation buffer. Captured material was removed from beads with 0.04 mL of Laemmli sample buffer, at 95°C for five minutes. Controls were carried out with either non-biotinylated 14-3-3 epsilon and GPx4 or GPx4 alone to rule out any unspecific binding to the beads. Samples were analyzed by Western Blotting.

Biotinylated 14-3-3ε (1.5 μg) or biotinylated GPx4 (500 ng) was incubated with HEK293T cytosol (0.15 mg) in 50 mM KH_2PO_4/K_2HPO_4, 50 mM KCl, 2.5 mM GSH and 0.05% (w/v) CHAPS, pH 7.0 for thirty minutes at 25°C. Sample were affinity purified as reported above and used for Western Blotting.

Expression of Hs 14-3-3ε in HEK293T cells

The pcDNA3.1 expression vector containing the full length human14-3-3ε sequence was from GenScript (Hong Kong, HK). HEK293Tcells were plated in a 6-well plate 24 hours before transfection and grown overnight to 50% confluency. *Trans*IT-LT1 reagent:DNA complex was prepared according to the manufacturer's instructions (Mirus Bio, LLC, WI, U.S.A.). Briefly, 2.5 μg of plasmid DNA were diluted in 0.25 mL Opti-MEM I Reduced Serum Media (Gibco, ThermoFisher Scientific, U.S.A) with 7.5 μL of TransIT®-LT1 reagent, kept at 25°C for 15 minutes, before adding to cells dropwise. After 48 hours from transfection, cells were harvested, washed with phosphate-buffered saline, centrifuged at 500xg for 5 minutes and the pellet was used for cytosol preparation.

Silencing of YWHAE gene in HEK293T cells

Two specific MISSION® Predesigned short-interfering RNA (siRNA), SASI_Hs02_00342252, and SASI_Hs02_00342253, from Merck KGaA, Darmstadt, Germany, were used for *YWHAE* silencing. Briefly, after splitting, cells were plated in 6 wells plates and grown overnight to 50% confluency. The next day, cells were kept in medium without serum and antibiotics for one hour before transfection. YWHAE siRNAs were diluted in 0.5 mL Opti-MEM I Reduced Serum Media (Gibco,

ThermoFisher Scientific, U.S.A), with 4 μL o Lipofectamine™ RNAiMAX (Invitrogen, ThermoFisher Scientific, U.S.A) and kept at room temperature for 15 minutes, before adding to cells. The final concentration of RNA duplex was 30 nM. 24 hours after transfection medium was replaced by with the full growth medium. Cells were harvested 48 hours after transfection, washed and centrifuged as described above. Pellet was used for cytosol preparation.

Western blot

Protein concentration was measured by the Bradford method using BSA as standard. Whole samples from pull-down experiments and different amounts of protein (2.5 - 5 micrograms) for overexpression and silencing experiments were separated on a 15% Laemmli gel and blotted onto nitrocellulose overnight. Anti 14-3-3 (pan) primary antibodies (8312) were from Cell Signaling Technology, Inc., U.S.A.; anti β-actin primary antibodies (A5481), anti-rabbit (A3937) and anti-mouse (A3562) secondary antibodies Alkaline Phosphatase linked or biotin (B7389) linked were from Merck KGaA, Darmstadt, Germany. Nitro-blue tetrazolium and 5-bromo-4-chloro-3'-indolyphosphate were used to detect the chromogenic signal of AP reaction. Images were acquired with Epson perfection V700 photo, dual lens system scanner.

Statistical analysis

Statistical analysis was performed with Graph Pad Prism 7, version 7.0e, Sept 2018. Data were analyzed by multiple t-test, one unpaired t-test per row and are presented as mean and standard deviation of the mean. $P<0.05$ was considered statistically significant.

RESULTS

Inactivation of purified GPx4 by RSL3 requires cytosol

In all the experiments the activity of RSL3 was always verified by testing its capacity to induce ferroptosis in cells.

Aiming to investigate details on the mechanism and kinetics of GPx4 inactivation by RSL3, we used the purified enzyme. Surprisingly, we did not observe the inactivation suggested by previous studies on cells in culture (11). As a matter of fact, purified GPx4 was inhibited by RSL3 only by extending incubation time up to 24 hours. In this case, the percentage of residual GPx4 activity was 63.2 ± 5.1, 46.9 ± 2.8, 27.1 ± 1.5 and 12.3 ± 0.3 respectively for 10, 50, 100 and 300 μM RSL3 in three independent experiments. Nearly identical results were obtained both in the

presence and in the absence of GSH and also with (1*R*,3*R*)-RSL3 diastereomer. This inactivation, therefore, was considered not specific.

Otherwise, in the presence of HEK293T cell cytosol an evident and reproducible inactivation of added GPx4 was observed, but only when cytosol was used within 2-3 hours from preparation. For more reproducible and all-day-long lasting results a reductant, either 2.5 mM GSH or TCEP, had to be added (Figure 1). The presence of a reductant in the inactivation test was not necessary to get the highest inactivation-permitting activity also when GPx4 was thoroughly reduced, freed of thiol and used within 3-4 hours. Under the standard conditions of the inactivation test (see infra) the residual GPx4 activity was 34.4% ± 1.3% when the enzyme was just reduced and 40.3% ±1.2 % after five hours from its reduction. For this reason, when comparing samples containing different amounts of GPx4, 2.5 mM TCEP or GSH was always present in the inactivation test, in order to keep reduced the endogenous enzyme, and thus sensitive to inactivation (22).

As the extent of the inactivation of GPx4 by RSL3 depends on cytosolic protein concentration, RSL3 concentration and incubation time (Figure 2, A-C), we standardized these parameters for cell cytosol as follows: 0.5 mg mL^{-1} proteins, 0.1 mM RSL3 and twenty minutes, at 25°C. Under these experimental conditions approximately 60-70% inactivation of GPx4 was reproducibly observed. Treatment of cytosolic proteins with diamide completely abolished the inactivation-permitting activity, which was fully restored if 2.5 mM TCEP (or GSH, not shown) was present in the inactivation test with diamide-treated cytosol. This evidence indicated that a thiol-disulfide transition of the permitting factor was required to inhibit GPx4 peroxidase activity by RSL3. Moreover, only RSL3, but not the (1*R,*3*R*)-RSL3 diastereomer was active (Figure 3).

The conditions used for these *in vitro* experiments are quite different from those adopted for cells, due to the intrinsic differences of experimental models (enzymology *vs* cell biology). Indeed, since different parameters impact on GPx4 inactivation by RSL3 *in vitro*, as shown in figure 2, the standardization of experimental conditions was a necessary constrain for the optimization of the enzymatic test.

For a quantitative evaluation of the activity that permits GPx4 inactivation by RSL3 in different rat organs we standardized the inactivation assay as reported above, but using 1.5 mg mL^{-1} protein concentration and defined the unit (U) of this activity as reported in Materials and Methods.

Thus, we could reliably compare different samples and found that cytosols from different rat tissues contain similar amounts of GPx4 inactivation-permitting activity, indicating that the factor required for GPx4 inactivation by RSL3 is ubiquitous. (Table 1).

When it was clear that GPx4 inactivation-permitting activity in cytosol was due to 14-3-3ε, we tested the correlation between protein expression and activity in tissues where the difference was maximal. This showed that higher activity is associated to higher expression (Figure S1).

The inactivation of GPx4 by RSL3 in the presence of HEK293T cell cytosol was observed not only with rat GPx4, but also with GPx4 purified form different species, namely human and pig (Table S1).

14-3-3 accounts for to the inactivation-permitting activity on GPx4 in the presence of RSL3

Preliminary experiments with centrifugal concentrators at different cut-off suggested that the activity permitting GPx4 inactivation by RSL3 was in the 50-100 kDa fraction. Treatment of the sample by heat or acid abolished the activity, confirming that a heat labile factor, seemingly a protein, was involved (not shown).

The stepwise purification of this protein was carried out first on HEK293T cells cytosol by ion exchange chromatography followed by size-exclusion chromatography. MS analysis of the chromatographic fraction containing the highest inactivation-permitting activity identified prothymosine α and different 14-3-3-isoforms as the most abundant species, on the basis of the exponentially modified protein abundance index (emPAI) of the proteomic software Mascot used. These MS data are reported as MS data 1_HEK293T in Supporting information. Similar results in terms of chromatographic behavior and MS identifications were obtained using rat kidney cytosol as source of the inactivation-permitting activity. However, tropomyosin α, but not prothymosine, and 14-3-3 isoforms were the most abundant identified proteins (MS data 1_Kidney in Supporting information). To further purify the inactivation-permitting activity we introduced another chromatographic step: we used, in sequence, hydrophobic interaction, ion exchange and size-exclusion chromatography. The flow chart of the purification from rat kidney cytosol is reported in Figure 4.

The final fractions from size-exclusion chromatography were analyzed by MS and the 14-3-3 isoforms ε, β/α, γ and τ were the most abundant species identified.

Proteomic data supporting the identification are available under Supporting information as MS data 2_Kidney.

Validation of the identification of 14-3-3 isoforms

Due to the large similarity among 14-3-3 proteins, we resorted to validating the MS identification using human recombinant 14-3-3ε, since this isoform had the highest identification score. The intact protein was produced in *E. Coli* using the pGEX-6P-1 expression vector, where the full length human 14-3-3ε sequence was cloned. This vector is engineered to produce the cloned protein linked to an N-terminal GST tag, used for the first affinity purification step and then removed.

Recombinant 14-3-3ε was first assayed to assess whether it could replace cytosol in permitting GPx4 inactivation by RSL3. Indeed, 14-3-3ε permits GPx4 inactivation by RSL3. This was not reproduced when the diastereomer (1*R,*3*R*)-RSL3 was used. During the whole purification protocol the protein was kept under reducing conditions and when freed from thiol it maintained its ability to permit GPx4 inactivation by RSL3 for several hours. Moreover, also 14-3-3ε failed to permit GPx4 inactivation by RSL3 when previously oxidized with diamide. Nevertheless, its inactivation-permitting activity was completely recovered when a reductant, either GSH or TCEP, was present during the incubation with GPx4 and RSL3 (Figure 5).

The inactivation of GPx4 by RSL3 depends on both 14-3-3ε and RSL3 concentrations (Figure 6).

As for HEK293T cell cytosol, also 14-3-3ε permits the inactivation of GPx4 purified from different species by RSL3 (Table S1).

14-3-3ε permits the RLS3-mediated alkylation of the selenocysteine moiety of GPx4

MS analysis of GPx4 inactivated by RSL3 in the presence of reduced 14-3-3ε showed that the catalytic selenium was covalently bound to RSL3 (Figure 7). This confirms the occurrence of a nucleophilic substitution reaction, with Cl^- as leaving group. This evidence validates the mechanism previously proposed, based on the observation that electrophilic chloroacetamide moiety of RSL3 is essential for its function (11).

GPx4 interacts with reduced 14-3-3ε only in the absence of RSL3

An affinity approach (23, 24) was used to demonstrate the interaction between GPx4 and 14-3-3ε. Briefly: reduced 14-3-3ε, labeled with a biotin tag, was incubated with the peroxidase in the presence and in the absence of RSL3. Streptavidin linked

to magnetic beads captured biotinylated 14-3-3ε and GPx4. Notably, the protein-protein interaction was clearly observed only in the absence of RSL3 (Figure 8, panel A lane 1), while in the presence of RSL3 it was hardly detectable (Figure 8, panel A lane 2). This evidence suggests that GPx4/14-3-3ε interaction is independent from RSL3 and that the alkylation of the catalytic selenocysteine reverts the affinity of the interaction.

Bioinformatic analysis using 14-3-3Pred tool (25) indicates a putative 14-3-3 binding motif (DWRCAR^{13}SMHEF) in GPx4. As there is no evidence for ^{13}S phosphorylation in purified GPx4 by MS analysis and the inhibition test works also in phosphate buffer, the involvement of this 14-3-3 binding motif is ruled out. Moreover, no structural elements on GPx4 molecular surface can fit the amphipatic groove on 14-3-3 proteins, differently from other binding partners. The involvement of the catalytic SeCys in binding to 14-3-3ε with the formation of a seleno-disulfide is seemingly excluded since inactivation-permitting activity of 14-3-3ε takes place in the presence of millimolar glutathione. Moreover, as high ionic strength decreases the permitting activity of 14-3-3ε on GPx4 inactivation by RSL3, an electrostatic interaction between the two proteins is the most likely mechanism.

This interaction was confirmed in HEK293T cell cytosol (Figure 8, panel B lane 1). Biotinylated GPx4 binds 14-3-3 proteins present in HEK293T cell cytosol quite effectively (Figure 8, panel C lane 1).

GPx4/14-3-3ε interaction does not affect GPx4 kinetics

To verify whether the interaction between GPx4 and 14-3-3ε had an effect on the function of the active site by impacting on protein dynamic during catalysis, we calculated the rate constants of individual steps of GPx4 reaction under steady-state conditions in the presence of 14-3-3ε (18).

For GPx4, the calculated k_{+1} was $1.51 \times 10^7 \pm 0.38 \times 10^7$ $M^{-1}s^{-1}$ and the k'_{+2} $7.57 \times 10^4 \pm 0.94 \times 10^4$ $M^{-1}s^{-1}$. These values did not change in presence of 14-3-3ε, k_{+1} resulting $1.38 \times 10^7 \pm 0.11 \times 10^7$ $M^{-1}s^{-1}$ and k'_{+2} $7.26 \times 10^4 \pm 2.13 \times 10^4$ $M^{-1}s^{-1}$. This observation rules out a significant impact of 14-3-3ε on kinetics of GPx4.

In HEK293T cells transient transfection and silencing of YWHAE gene, coding for 14-3-3ε, affect cytosol inactivation-permitting activity of GPx4 by RSL3

In order to investigate the effect of the overexpression of 14-3-3ε in HEK293T cells on GPx4 inactivation by RSL3 we transfected HEK293T cells with a vector containing the cDNA ORF of human 14-3-3ε and with the empty vector for controls.

Overexpression of 14-3-3ε was confirmed by WB (Figure 9, panel A). We measured GPx4 inactivation by RSL3 in the presence of cell cytosols at three different protein concentrations, 0.38, 1.14 and 2.28 mg mL^{-1}, and four different RSL3 concentrations, 0.1, 1, 10 and 100 μM. Each experiment was performed in three replicates. A significant difference was detectable with 1 μM RSL3 and 1.14 mg mL^{-1} protein concentration (residual GPx4 activity: 99.1% ± 0.8% in controls and 91.6% ± 1.4% in cells overexpressing 14-3-3ε, $p<0.01$) and 2.28 mg mL^{-1} protein concentration (residual GPx4 activity: 98.2% ± 1.4% in controls and 92.7% ± 1.7% in cells overexpressing 14-3-3ε, $p=0.012$). Moreover, with 10 μM RSL3 a higher GPx4 inactivation with cytosol of cells overexpressing 14-3-3ε was detectable at all the protein concentrations used (Figure 9, panel B). This result with 10 μM RSL3 was confirmed with three different transfection experiments using 1.1 mg mL^{-1} protein concentration: the amount of GPx4 inactivation was 77.7% ± 0.8% and 70.1 ± 1.2% with cytosols from cell transfected with the empty vector and with 14-3-3ε vector, respectively ($p<0.001$).

Silencing of *YWHAE* gene was confirmed by RT-PCR (not shown) and at protein level by WB (Figure 9, panel C). GPx4 inactivation by 0.1 mM RSL3 was measured in the presence of cytosols from control (scrambled) cells and *YWHAE* silenced cells (si14-3-3) after 48 hours from transfection. Three protein concentration were tested: 0.1, 0.25 and 0.5 mg mL^{-1}. As shown in Figure 9, panel D, a significant difference ($p<0.0001$) was seen with 0.25 and 0.5 mg mL^{-1}, while no difference was detected with the lowest protein concentration used (0.1 mg mL^{-1}).

Though beyond the specific aims of the present paper, we carried out experiments with HEK293T cells either transiently overexpressing 14-3-3ε or silenced for this protein to test whether there was a clear modulation of ferroptosis induced by RSL3. Anyway, likely due to compensatory mechanisms, our experiments led to inconclusive results.

DISCUSSION

Compelling evidence supports the notion that the missing activity of GPx4 leads to a peculiar form of regulated cell death, named ferroptosis (11, 12, 26). Although other constraints, such as membrane fatty acid composition and iron availability must be fulfilled, it is the insufficient reduction of lipid hydroperoxides, from which lipid peroxidation is activated, the critical event priming ferroptosis (13,

14). Consistent with the notion of “regulated”, the execution of cell death by ferroptosis evolves through a patterned morphological pathway (16, 27, 28). In this perspective, compounds targeting GPx4 activity can be seen as agonists in the frame of an ordered process. The present evidence that the adaptor protein 14-3-3ε is indispensable to the inactivation of GPx4, contributes in supporting the view that GPx4 inactivation can be seen as a physiologically controlled event. Ferroptosis can be framed in the overall scenario of tissue plasticity encompassing proliferation, differentiation and death (29, 30). In this perspective, we do not know which is the physiological agonist that could mimic the electrophile RSL3.

Our data show that GPx4 interacts with the electrophilic compound only following the interaction with the adaptor protein, in a reduced form. It is only following this interaction, indeed, that alkylation of the catalytic selenocysteine is possible and inactivates the enzyme. Our observations also indicate that, upon this event, it is the alkylated, inactive peroxidase that loses affinity for the adaptor protein. The interaction of 14-3-3 proteins with target proteins underlies different effects. Among them, a conformational change seems the one which could give an account for the activity of 14-3-3ε on permitting GPx4 inactivation by RSL3: upon binding to 14-3-3ε GPx4 undergoes a conformational shift which makes it more prone to react with RSL3, so that the enzyme is inactivated. At the same time, the reaction of the electrophile with the catalytic selenocysteine itself or with other cysteine residues promotes another conformational shift which weakens GPx4 affinity for 14-3-3ε.

The notion that the inactivation of GPx4 by RSL3 permitted by 14-3-3ε requires that the adaptor protein is reduced confirms the already known redox regulation of 14-3-3 proteins (31, 32). Physiologically, the necessity of reduced adaptor to permit the inactivation of GPx4 by an electrophile, is reminiscent of a complex homeostatic scenario. In fact, a less nucleophilic environment, e.g. cells under GSH depletion, might contribute to supporting homeostasis by protecting GPx4 against inactivation due to a still unknown electrophile. All together these considerations, although at the moment only speculative, are evocative of a redox homeostasis operating by fine feedback mechanisms, extended to cell death and survival, of which GPx4 is a pivotal, regulated player.

A reproducibly high inactivation-permitting activity was detectable in cells overexpressing 14-3-3ε. Consistently, silencing of *YWHAE* gene also affected cytosol inactivation-permitting activity, though in finite way. The limited effect is

seemingly due to the rescuing of the biological activity of 14-3-3ε by the other isoforms.

The adaptor 14-3-3 proteins are involved in several cellular processes, usually connected to signaling pathways. Seven mammalian 14-3-3 isoforms exist (α/β, γ, σ, δ/ζ, η, ε, and τ), most frequently arranged in dimeric form. The rich set of dimer combinations implies a large monomer exchange, expanding the repertory of 14-3-3 interactions (33). On the other hand, although dimeric forms of 14-3-3 proteins dominate, monomers can be also present and functionally active under specific conditions (34). As expression of different isoforms is dispensable, likely different isoforms complement each other (35), thus possibly accounting for the limited result of our silencing experiment. This could also be the reason why the biological validation in cells of modulation of the expression of 14-3-3ε on ferroptosis was not positively achieved.

It is generally accepted that interactions between 14-3-3 proteins and target proteins underlie different biochemical effects, such as modifying conformation, masking a specific region of the target or scaffolding with other molecules (36). The last seems the mechanism involved in GPx4 inactivation by RSL3. Our results indicate that GPx4 binds to 14-3-3ε independently from the presence of the electrophile, thus opening new, exciting perspectives in understanding how GPx4 activity is regulated in cells. The observation that such an interaction does not affect GPx4 kinetics apparently rules out conformational stabilizations influencing the catalytic activity.

Although a number of different motifs were identified in proteins that bind to 14-3-3 proteins (37), it is now well known that the presence of these recognized motifs it is not strictly necessary for interaction. This is the case for another selenoprotein, Selenoprotein W, which interacts with 14-3-3β but neither contains any of the high-affinity 14-3-3 binding motifs, nor presents any phosphorylated serine or threonine (38, 39).

Post-translational modifications, including phosphorylation, acetylation, and oxidation (31, 31, 37) may affect 14-3-3 proteins binding capability.

In conclusion, the fact that only reduced 14-3-3ε permits GPx4 inactivation by RSL3 highlights a redox dependency of this inactivation in the frame of redox homeostasis and signaling.

ACKNOWLEDGEMENTS

This work was supported by the University of Padova, Progetti di Ricerca di Ateneo, CPDA151400/15 to MM and by HFSP (RGP0013/2014) to F.U. Funding sources were not involved in the conduct of the research.

REFERENCES

1. Maiorino, M., Gregolin, C., and Ursini, F. (1990) Phospholipid hydroperoxide glutathione peroxidase. *Meth. Enzymol*. 186, 448-457

2. Maiorino, M., Coassin, M., Roveri, A., and Ursini, F. (1989) Microsomal lipid peroxidation: effect of vitamin E and its functional interaction with phospholipid hydroperoxide glutathione peroxidase. *Lipids* **24**, 721-726

3. Yang, W. S., and Stockwell, B. R. (2008) Synthetic lethal screening identifies compounds activating iron-dependent, nonapoptotic cell death in oncogenic-RAS-harboring cancer cells. *Chem. Biol*. 1**5**, 234-245

4. Dolma, S., Lessnick, S. L., Hahn, W. C., and Stockwell, B. R. (2003) Identification of genotype-selective antitumor agents using synthetic lethal chemical screening in engineered human tumor cells. *Cancer Cell* **3**, 285-296

5. Dixon, S. J., Lemberg, K. M., Lamprecht, M. R., Skouta, R., Zaitsev, E. M., Gleason, C. E., Patel, D. N., Bauer, A. J., Cantley, A. M., Yang, W. S., Morrison, B., 3rd, and Stockwell, B. R. (2012) Ferroptosis: an iron-dependent form of nonapoptotic cell death. *Cell* **149**, 1060-1072

6. Dixon, S. J., and Stockwell, B. R. (2014) The role of iron and reactive oxygen species in cell death. *Nat. Chem. Biol*. **10**, 9-17

7. Conrad, M., and Sato, H. (2012) The oxidative stress-inducible cystine/glutamate antiporter, system x (c) (-) : cystine supplier and beyond. *Amino Acids* **42**, 231-246

8. Yagoda, N., von Rechenberg, M., Zaganjor, E., Bauer, A. J., Yang, W. S., Fridman, D. J., Wolpaw, A. J., Smukste, I., Peltier, J. M., Boniface, J. J., Smith, R., Lessnick, S. L., Sahasrabudhe, S., and Stockwell, B. R. (2007) RAS-RAF-MEK-dependent oxidative cell death involving voltage-dependent anion channels. *Nature* **447**, 864-868

9. Yant, L. J., Ran, Q., Rao, L., Van Remmen, H., Shibatani, T., Belter, J. G., Motta, L., Richardson, A., and Prolla, T. A. (2003) The selenoprotein GPX4 is essential for mouse development and protects from radiation and oxidative damage insults. *Free Radic. Biol. Med*. **34**, 496-502

10. Liang, H., Yoo, S. E., Na, R., Walter, C. A., Richardson, A., and Ran, Q. (2009) Short form glutathione peroxidase 4 is the essential isoform required for survival and somatic mitochondrial functions. *J. Biol. Chem*. **284**, 30836-30844

11. Yang, W. S., SriRamaratnam, R., Welsch, M. E., Shimada, K., Skouta, R., Viswanathan, V. S., Cheah, J. H., Clemons, P. A., Shamji, A. F., Clish, C. B., Brown, L. M., Girotti, A. W., Cornish, V. W., Schreiber, S. L., and Stockwell, B. R. (2014) Regulation of ferroptotic cancer cell death by GPX4. *Cell* **156**, 317-331

12. Friedmann Angeli, J. P., Schneider, M., Proneth, B., Tyurina, Y. Y., Tyurin, V. A., Hammond, V. J., Herbach, N., Aichler, M., Walch, A., Eggenhofer, E., Basavarajappa, D., Radmark, O., Kobayashi, S., Seibt, T., Beck, H., Neff, F., Esposito, I., Wanke, R., Forster, H., Yefremova, O., Heinrichmeyer, M., Bornkamm, G. W., Geissler, E. K., Thomas, S. B., Stockwell, B. R., O'Donnell, V. B., Kagan, V. E., Schick, J. A., and Conrad, M. (2014) Inactivation of the ferroptosis regulator Gpx4 triggers acute renal failure in mice. *Nat. Cell. Biol.* **16**, 1180-1191

13. Feng, H., and Stockwell, B. R. (2018) Unsolved mysteries: How does lipid peroxidation cause ferroptosis? *PLoS Biol.* **16**, e2006203

14. Maiorino, M., Conrad, M., and Ursini, F. (2018) GPx4, Lipid Peroxidation, and Cell Death: Discoveries, Rediscoveries, and Open Issues. *Antioxid. Redox Signal*. **29**, 61-74

15. Lu, B., Chen, X. B., Ying, M. D., He, Q. J., Cao, J., and Yang, B. (2017) The Role of Ferroptosis in Cancer Development and Treatment Response. *Front. Pharmacol.* **8**, 992

16. Stockwell, B. R., Friedmann Angeli, J. P., Bayir, H., Bush, A. I., Conrad, M., Dixon, S. J., Fulda, S., Gascon, S., Hatzios, S. K., Kagan, V. E., Noel, K., Jiang, X., Linkermann, A., Murphy, M. E., Overholtzer, M., Oyagi, A., Pagnussat, G. C., Park, J., Ran, Q., Rosenfeld, C. S., Salnikow, K., Tang, D., Torti, F. M., Torti, S. V., Toyokuni, S., Woerpel, K. A., and Zhang, D. D. (2017) Ferroptosis: A Regulated Cell Death Nexus Linking Metabolism, Redox Biology, and Disease. *Cell* **171**, 273-285

17. Roveri, A., Maiorino, M., Nisii, C., and Ursini, F. (1994) Purification and characterization of phospholipid hydroperoxide glutathione peroxidase from rat testis mitochondrial membranes. *Biochim. Biophys. Acta* **1208**, 211-221

18. Ursini, F., Maiorino, M., and Gregolin, C. (1985) The selenoenzyme phospholipid hydroperoxide glutathione peroxidase. *Biochim. Biophys. Acta* **839**, 62-70

19. Allen, G. (1986) Sequencing of proteins and peptides. in Laboratory techniques in biochemistry and molecular biology (T.S., W., and Burdon, R. eds.), 3rd Ed., Elsevier Science, Amsterdam, the Netherlands. pp 30-31

20. Dalziel, K. (1957) Initial Steady State Velocities in the Evaluation of Enzyme-Coenzyme-Substrate Reaction Mechanisms. in *Acta Chemica Scandinavica* **11**(**10**), 1706-1723

21. Sztajer, H., Gamain, B., Aumann, K. D., Slomianny, C., Becker, K., Brigelius-Flohé, R., and Flohé, L. (2001) The putative glutathione peroxidase gene of Plasmodium falciparum codes for a thioredoxin peroxidase. *J. Biol. Chem*. **276**, 7397-7403

22. Orian, L., Mauri, P.L., Roveri, A., Toppo, S., Benazzi, L., Bosello-Travain, V., De Palma, A., Maiorino, M., Miotto, G., Zaccarin, M., Polimeno, A., Flohé, L., Ursini, F. (2015) Selenocysteine oxidation in glutathione peroxidase catalysis: an MS-supported quantum mechanics study. *Free Rad. Biol. Med*. **87**, 1-14

23. Podobnik, M., Krasevec, N., Zavec, A. B., Naneh, O., Flasker, A., Caserman, S., Hodnik, V., and Anderluh, G. (2016) How to Study Protein-protein Interactions. *Acta Chimica Slovenica* **63**, 424-439

24. Hermanson, G. T. (1996) Bioconjugate Techniques, Academic Press, London, UK

25. Madeira, F., Tinti, M., Murugesan, G., Berret, E., Stafford, M., Toth, R., Cole, C., MacKintosh, C., and Barton, G.J. (2015) 14-3-3Pred: improved methods to predict 14-3-3 binding peptides. *Bioinformatics* 31(14), 2276-2283

26. Hirschhorn, T., and Stockwell, B. R. (2018) The development of the concept of ferroptosis. *Free Radic. Biol. Med*. 10.1016/j.freeradbiomed.2018.09.043

27. Conrad, M., Kagan, V. E., Bayir, H., Pagnussat, G. C., Head, B., Traber, M. G., and Stockwell, B. R. (2018) Regulation of lipid peroxidation and ferroptosis in diverse species. *Genes Dev*. **32**, 602-619

28. Lewerenz, J., Ates, G., Methner, A., Conrad, M., and Maher, P. (2018) Oxytosis/Ferroptosis-(Re-) Emerging Roles for Oxidative Stress-Dependent Non-apoptotic Cell Death in Diseases of the Central Nervous System. *Front. Neurosci*. **12**, 214

29. Wang, D., Xie, N., Gao, W., Kang, R., and Tang, D. (2018) The ferroptosis inducer erastin promotes proliferation and differentiation in human peripheral blood mononuclear cells. *Biochem. Biophys. Res. Commun*. **503**, 1689-1695

30. Gascón, S., Murenu, E., Masserdotti, G., Ortega, F., Russo, G. L., Petrik, D., Deshpande, A., Heinrich, C., Karow, M., Robertson, S. P., Schroeder, T., Beckers, J., Irmler, M., Berndt, C., Angeli, J. P. F., Conrad, M., Berninger, B., and Götz, M. (2016) Identification and successful negotiation of a metabolic checkpoint in direct neuronal reprogramming. *Cell Stem Cell* **18**, 396-409

31. Maheswaranathan, M., Gole, H. K., Fernandez, I., Lassegue, B., Griendling, K. K., and San Martin, A. (2011) Platelet-derived growth factor (PDGF) regulates Slingshot phosphatase activity via Nox1-dependent auto-dephosphorylation of serine 834 in vascular smooth muscle cells. *J. Biol. Chem*. **286**, 35430-35437

32. Kim, H. S., Ullevig, S. L., Nguyen, H. N., Vanegas, D., and Asmis, R. (2014) Redox regulation of 14-3-3zeta controls monocyte migration. *Arterioscler. Thromb. Vasc. Biol*. **34**, 1514-1521

33. Sluchanko, N. N., and Gusev, N. B. (2017) Moonlighting chaperone-like activity of the universal regulatory 14-3-3 proteins. *FEBS J*. **284**, 1279-1295

34. Sluchanko, N. N., and Gusev, N. B. (2012) Oligomeric structure of 14-3-3 protein: what do we know about monomers? *FEBS Lett.* **586**, 4249-4256

35. Steinacker, P., Schwarz, P., Reim, K., Brechlin, P., Jahn, O., Kratzin, H., Aitken, A., Wiltfang, J., Aguzzi, A., Bahn, E., Baxter, H. C., Brose, N., and Otto, M. (2005) Unchanged survival rates of 14-3-3gamma knockout mice after inoculation with pathological prion protein. *Mol. Cell. Biol*. **25**, 1339-1346

36. Bridges, D., and Moorhead, G. B. (2004) 14-3-3 proteins: a number of functions for a numbered protein. *Sci. STKE* 2004, re10

37. Aitken, A. (2011) Post-translational modification of 14-3-3 isoforms and regulation of cellular function. *Semin. Cell Dev. Biol*. **22**, 673-680

38. Musiani, F., Ciurli, S., and Dikiy, A. (2011) Interaction of selenoprotein W with 14-3-3 proteins: a computational approach. *J. Proteome Res*. **10**, 968-976

39. Jeon, Y. H., Ko, K. Y., Lee, J. H., Park, K. J., Jang, J. K., and Kim, I. Y. (2016) Identification of a redox-modulatory interaction between selenoprotein W and 14-3-3 protein. *Biochim. Biophys. Acta* **1863**, 10-18

Table 1. GPx4 inactivation-permitting activity by RSL3 in cytosol of different rat organs.

ORGAN	U/mg protein§
Adrenal	28.7 ± 0.4
Liver	27.0 ± 3.9
Ovary	22.7 ± 0.2
Spleen	22.0 ± 0.1
Brain	21.9 ± 1.1
Kidney	20.5 ± 0.2
Testis	19.7 ± 0.3
Heart	17.3 ± 0.7
Lung	16.7 ± 0.1
Small intestine	15.0 ± 1.3

Results are expressed as units of inactivation-permitting activity by milligram of protein: one inactivation-permitting unit (U) is defined as the amount of activity present in a sample yielding 50% GPx4 inactivation by RSL3, under the standardized conditions detailed under materials and methods.

§ mean and standard deviation of the mean for four independent experiments.

FIGURES LEGENDS

Figure 1. Inactivation-permitting activity of HEK293T cytosol decreases with time. Fresh cytosol was divided into two halves and 2.5 mM TCEP or the same volume of HB was added. At different times, the inactivation of freshly reduced GPx4 by 0.1 mM (1*S*, 3*R*)-RLS3 was performed in the presence of 0.25 mg mL^{-1} HEK293T cytosolic proteins for 20 minutes. The results are expressed as the percentage of residual enzyme activity in RSL3 treated samples *vs* the corresponding blanks treated with solvent. Each point is the mean and the standard deviation of the mean of three independent experiments.

Figure 2. Determinants of HEK293T cell cytosol and GPx4 inactivation by RSL3 All the inactivation tests contained a fixed concentration (50 nM) of freshly reduced GPx4 and were performed at 25°C. The other parameters, i.e protein and RSL3 concentrations and time, were varied one at a time, keeping the other two fixed: protein concentration 0.5 mg mL^{-1}; RSL3 concentration 0.1 mM and time 20 minutes. Effects of: A- concentration of HEK293T proteins (0.1 to 1.5 mg mL^{-1}); B- incubation time (10 to 80 minutes); C- RSL3 concentrations (0.1 μM to 0.3 mM). The results are expressed as the percentage of residual enzyme activity in RSL3 treated samples *vs* the corresponding blanks. Each point is the mean and the standard deviation of the mean of three independent experiments.

Figure 3. **HEK293T cell cytosol and GPx4 inactivation by RSL3: effect of thiols** Purified GPx4 was fully reduced, freed from thiol and used within three hours diluted to 50 nM in homogenizing buffer or in HEK293T cytosol (0.5 mg mL^{-1}). Diamide treated cytosol (0.5 mg mL^{-1}) indicates that HEK293T cytosol was incubated with diamide and freed from the thiol-oxidizing agent before the experiment. RSL3 diastereomer concentration was 0.1 mM. When present, the reductant concentration during the inactivation test was 2.5 mM. Results are expressed as the percentage of residual GPx4 activity in treated samples and are the mean and the standard deviation of the mean of three independent experiments.

Figure 4. **Purification of the protein permitting GPx4 inactivation by RSL3 from rat kidney cytosol.**

GPx4 inactivation-permitting activity was purified from rat kidney cytosol by a three-step chromatographic protocol. The red columns in each chromatogram indicate the

fractions containing the highest amount of inactivation-permitting activity, which were processed in the next step. Step A- proteins (0.1 g) were resolved by hydrophobic interaction chromatography (phenyl-sepharose). Step B- the fraction eluted at the lowest ammonium sulphate concentration was further separated using an ion exchange chromatography (MonoQ) by a stepwise gradient from 0.25 M to 1 M NaCl. Step C- proteins eluting at 300 mM NaCl ionic strength contained the highest inactivation-permitting activity and were resolved using a size exclusion chromatography (Superdex™ 75 10/300 GL).

Figure 5. **GPx4 inactivation by RSL3 requires reduced 14-3-3ε and is stereospecific.**

GPx4 (50 nM) and recombinant 14-3-3ε (0.5 μM) both reduced and freed from thiol were immediately used. Each sample was divided in two aliquots and incubated either with 0.1 mM of the specified diastereomer (treated) or solvent (blank). Diamide treated 14-3-3ε (0.5 μM) indicates that 14-3-3ε was incubated with diamide and freed from the thiol-oxidizing agent before the experiment. When present, the reductant concentration during the inactivation test was 2.5 mM. The results are expressed as the percentage of residual GPx4 activity in treated samples and are the mean and the standard deviation of the mean of three independent experiments.

Figure 6. GPx4 inactivation by RSL3 is 14-3-3ε and RSL3 concentrations dependent.

Purified GPx4 (50 nM) was added to different concentrations (indicated with different colors) of reduced recombinant 14-3-3ε. Aliquots of each mixture were incubated with different RSL3 concentrations (0.1 μM, 1 μM and 10 μM) or solvent for blanks at 25°C. GPx4 activity was measured after 20 minutes. Controls were carried out in the absence of 14-3-3ε. The results are expressed as percentage of the residual activity of RSL3-treated *vs* blank sample. Data are the mean and the standard deviation of the mean of three independent experiments.

Figure 7. **SeCys of GPx4 is alkylated by RSL3.**

Reduced 14-3-3ε and GPx4 were incubated in the presence of 0.1 mM RSL3 for 20 minutes before carboxymethylation and hydrolysis. Tryptic fragments were analyzed by MS. A: tandem mass spectrum of the fragment corresponding to $T_{34\text{-}48}$ tryptic

peptide harboring one RSL3 species and two carboxymethylation. B: the identified sequence GC$^{(IA)}$VC$^{(IA)}$IVTNVASQU$^{(RSL3)}$GK, shows SeCys46 covalently bound to RSL3 and carboxymethylation on Cys35 and Cys37.

Figure 8. **Interaction between recombinant 14-3-3ε and GPx4**.

Reduced biotinylated 14-3-3ε and purified GPx4 interact and are pulled down together (Panel A, lane 1). The presence of 0.2 mM (*1S, 3R*)-RSL3 inhibits their interaction (Panel A, lane 2). Panel B: biotinylated 14-3-3ε binds GPx4 present in HEK293T cell cytosol (lane 1); biotin-linked secondary antibodies and streptavidin-alkaline phosphatase conjugate are used. Panel C: biotinylated GPx4 interacts with 14-3-3 proteins of HEK293T cytosol. Unspecific binding of 14-3-3ε and GPx4 to beads was never detected.

Figure 9. Overexpression of 14-3-3ε and silencing of *YWHAE* gene impacts on inactivation-permitting activity of HEK293T cytosol.

Overexpression of 14-3-3ε in HEK293T cells was tested by WB (Panel A- 2.5 μg protein; lane 1: empty vector, lane 2: 14-3-3ε vector). Panel B: purified GPx4 (50 nM) was added to different protein concentrations of cytosol from HEK293T cells transfected with the empty vector (red circles) and with the 14-3-3ε vector (blue triangles) and treated with 10 μM RSL3. GPx4 inactivation is significantly higher where 14-3-3ε is overexpressed. Silencing of *YWHAE* gene was confirmed by WB (Panel C- 5 μg protein; lane 1: scrambled, lane 2: si14-3-3ε). Panel D: 50 nM GPx4 was incubated with 0.1 mM RSL3 in the presence of different protein concentrations from cytosol of control HEK293T cells (red diamonds) and si14-3-3ε HEK293T cells (blue circles). A significantly lower GPx4 inactivation was measured with 0.25 and 0.5 mg mL^{-1} si14-3-3ε HEK293T cell cytosol. Data are the mean and standard deviation of the mean of three and four replicates for overexpression and silencing experiments, respectively.

*: $p<0.01$; **: $p<0.001$ and ***: $p<0.0001$.

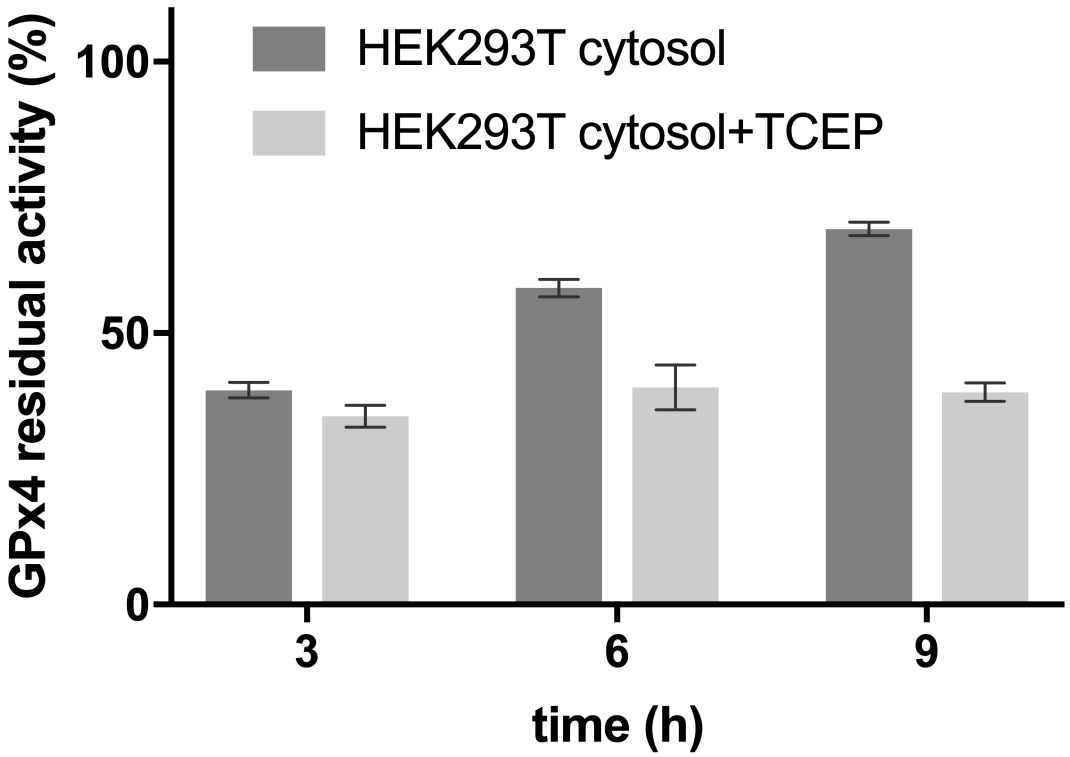
GPx4 residual activity (%)
100
50
0
HEK293T cytosol
HEK293T cytosol+TCEP
3
6
9
time (h)

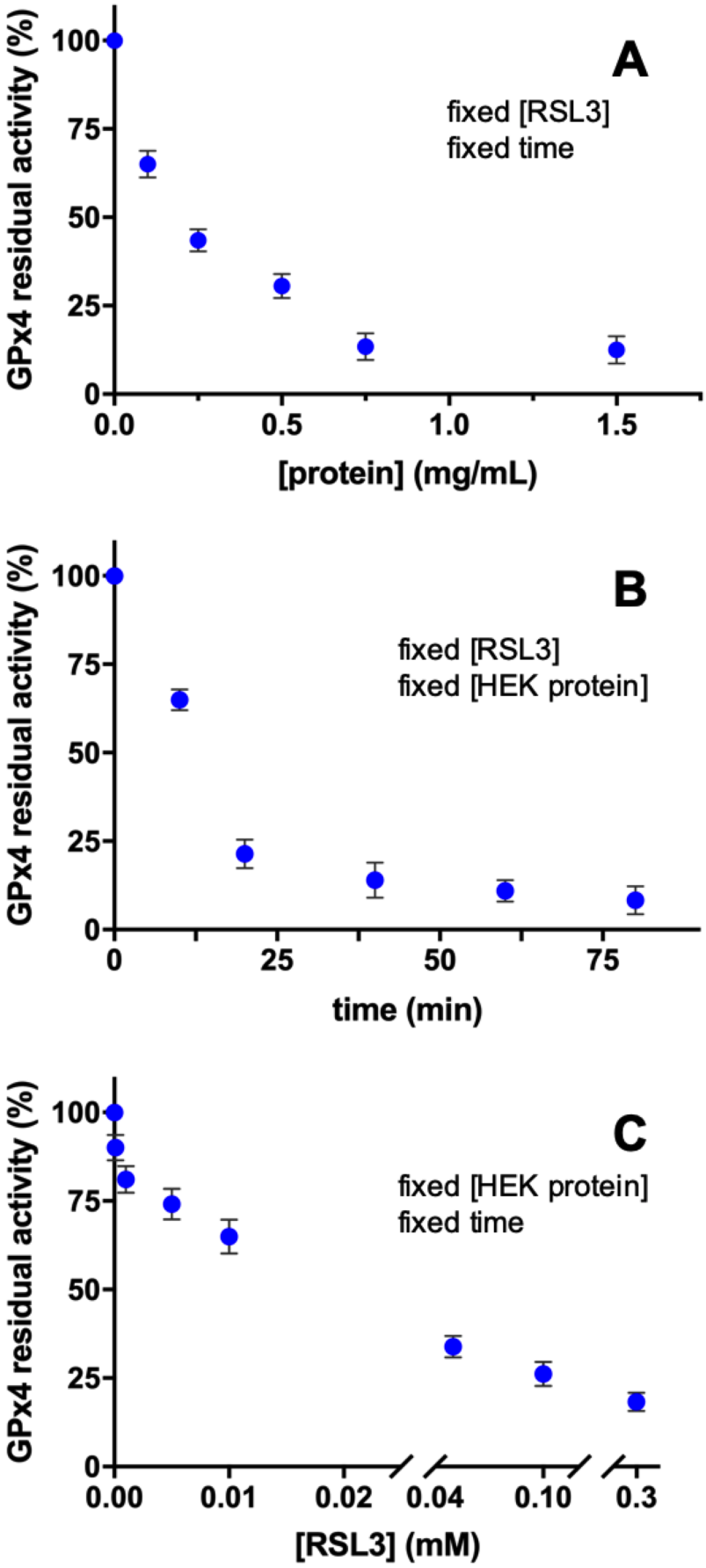
A
fixed [RSL3]
fixed time
GPx4 residual activity (%)
100
75
50
25
0
0.0
0.5
1.0
1.5
[protein] (mg/mL)
B
fixed [RSL3]
fixed [HEK protein]
GPx4 residual activity (%)
100
75
50
25
0
0
25
50
75
time (min)
C
fixed [HEK protein]
fixed time
GPx4 residual activity (%)
100
75
50
25
0
0.00
0.01
0.02
0.04
0.10
0.3
[RSL3] (mM)

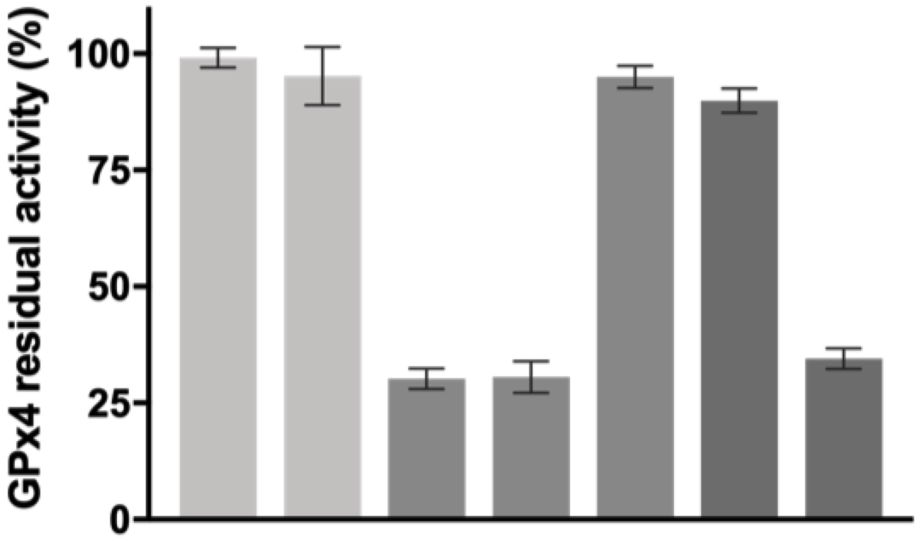

GPx4	+	+	+	+	+	+	+
cytosol	-	-	+	+	+	-	-
diamide treated cytosol	-	-	-	-	-	+	+
GSH	-	+	-	-	-	-	-
TCEP	-	-	-	+	+	-	+
(1S,3R)-RSL3	+	+	+	+	-	+	+
(1R,3R)-RSL3	-	-	-	-	+	-	-

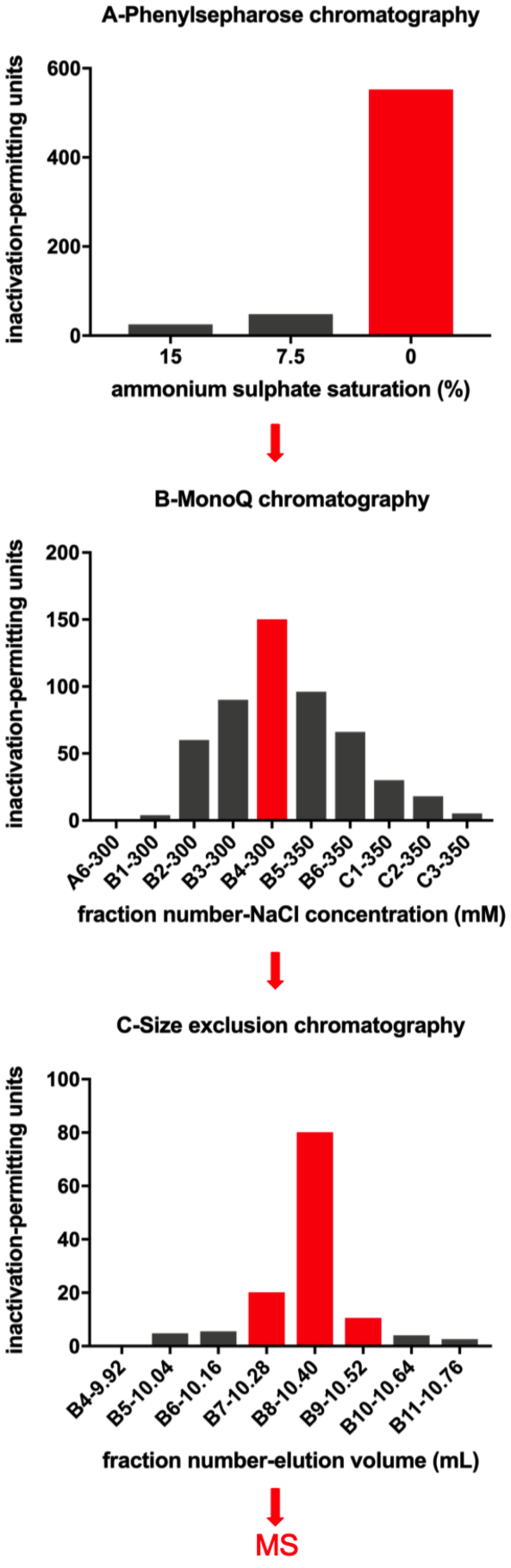
A-Phenylsepharose chromatography
inactivation-permitting units
600
400
200
0
15
7.5
0
ammonium sulphate saturation (%)
B-MonoQ chromatography
inactivation-permitting units
200
150
100
50
0
A6-300
B1-300
B2-300
B3-300
B4-300
B5-350
B6-350
C1-350
C2-350
C3-350
fraction number-NaCl concentration (mM)
C-Size exclusion chromatography
inactivation-permitting units
100
80
60
40
20
0
B4-9.92
B5-10.04
B6-10.16
B7-10.28
B8-10.40
B9-10.52
B10-10.64
B11-10.76
fraction number-elution volume (mL)
MS

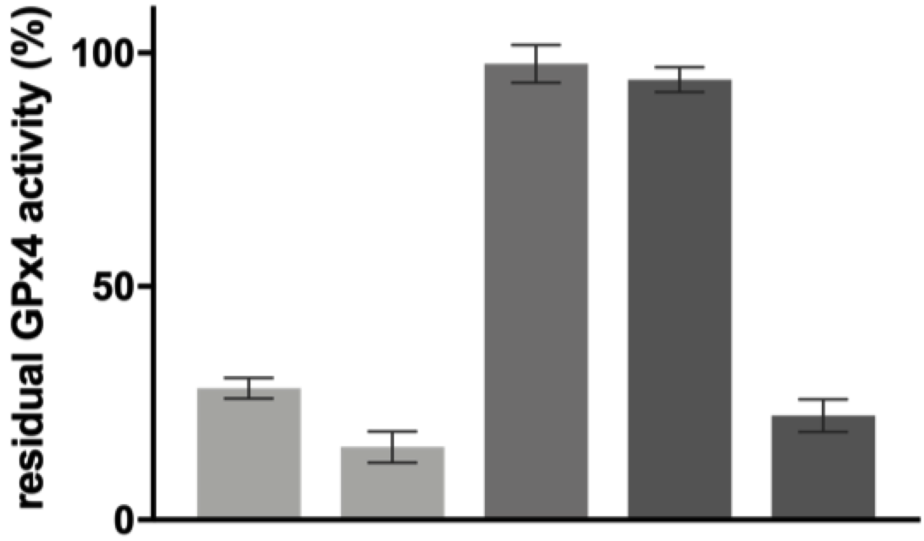

GPx4	+	+	+	+	+
14-3-3ε	+	+	+	-	-
diamide treated 14-3-3ε	-	-	-	+	+
TCEP	-	+	+	-	+
(1S,3R)-RSL3	+	+	-	+	+
(1R,3R)-RSL3	-	-	+	-	-

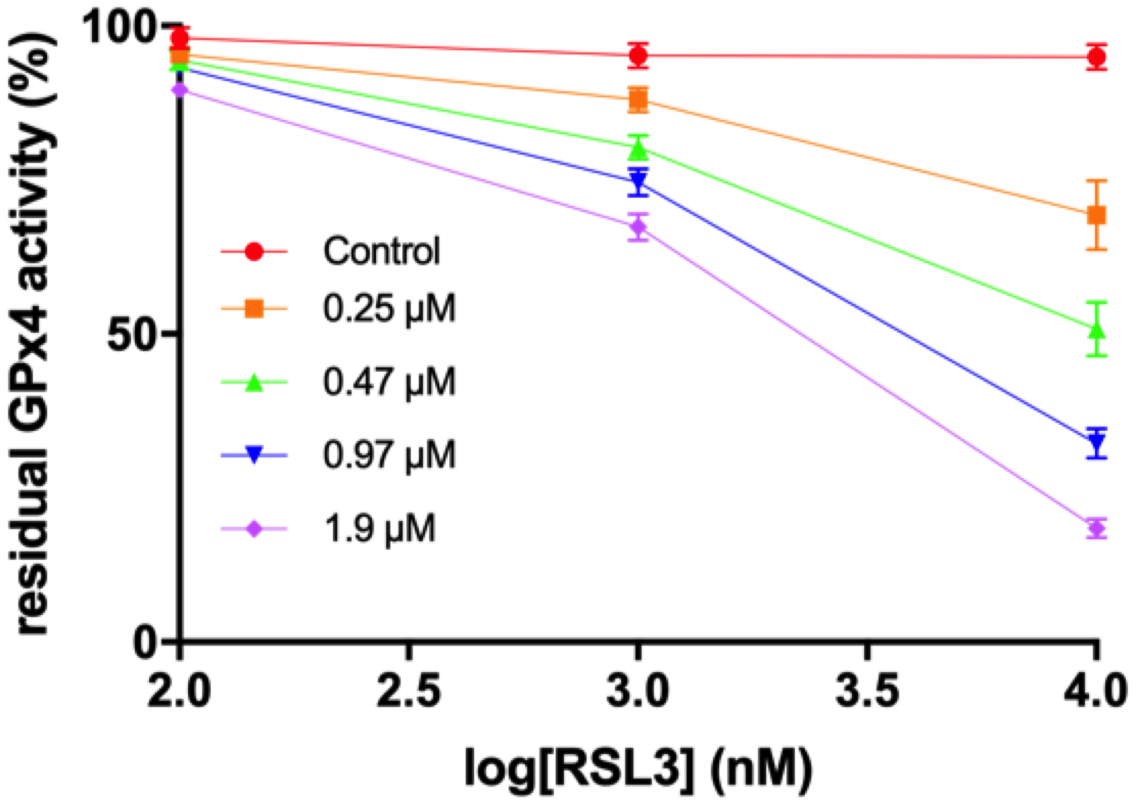
residual GPx4 activity (%)
100
50
0
2.0
2.5
3.0
3.5
4.0
log[RSL3] (nM)
Control
0.25 μM
0.47 μM
0.97 μM
1.9 μM

MS/MS of T_{34-48}: GC$^{(IA)}$VC$^{(IA)}$IVTNVASQU$^{(RSL3)}$GK

A

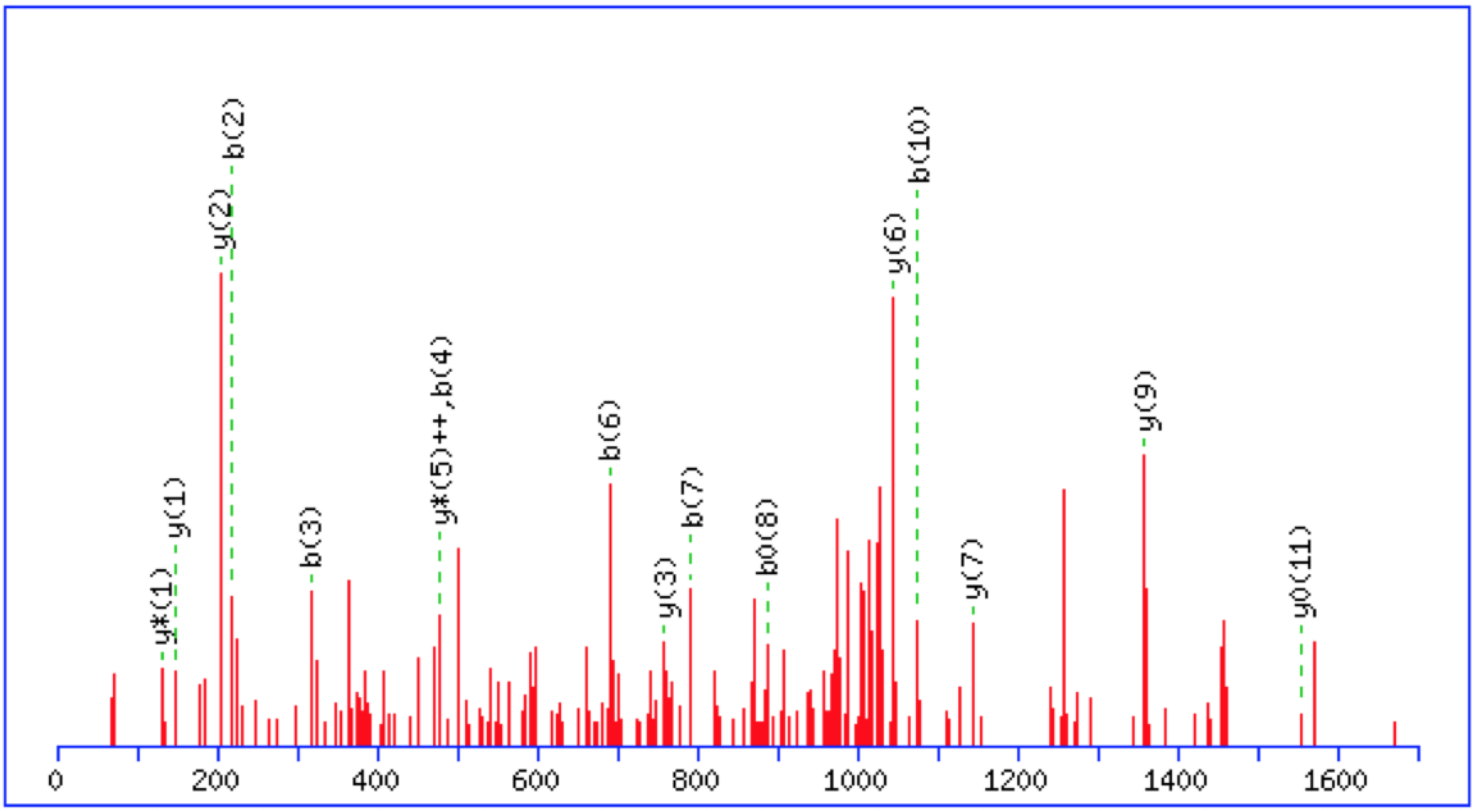

B

#	b	b^{++}	b*	b^{*++}	b^{0}	b^{0++}	Seq.	y	y^{++}	y*	y^{*++}	y^{0}	y^{0++}	#
1	58.0287	29.5180					G							15
2	***219.0434***	110.0253					C	1992.7621	996.8847	1975.7355	988.3714	1974.7515	987.8794	14
3	***318.1118***	159.5595					V	1831.7474	916.3773	1814.7209	907.8641	1813.7369	907.3721	13
4	***479.1265***	240.0669					C	1732.6790	866.8431	1715.6525	858.3299	1714.6684	857.8379	12
5	592.2105	296.6089					I	1571.6643	786.3358	1554.6378	777.8225	1553.6538	777.3305	11
6	***691.2790***	346.1431					V	1458.5803	729.7938	1441.5537	721.2805	1440.5697	720.7885	10
7	***792.3266***	396.6670			774.3161	387.6617	T	***1359.5119***	680.2596	1342.4853	671.7463	1341.5013	671.2543	9
8	906.3696	453.6884	889.3430	445.1751	888.3590	444.6831	N	1258.4642	629.7357	1241.4376	621.2225	1240.4536	620.7304	8
9	1005.4380	503.2226	988.4114	494.7094	987.4274	494.2173	V	***1144.4213***	572.7143	1127.3947	564.2010	1126.4107	563.7090	7
10	***1076.4751***	538.7412	1059.4485	530.2279	1058.4645	529.7359	A	***1045.3528***	523.1801	1028.3263	514.6668	1027.3423	514.1748	6
11	1163.5071	582.2572	1146.4806	573.7439	1145.4966	573.2519	S	974.3157	487.6615	957.2892	479.1482	956.3052	478.6562	5
12	1291.5657	646.2865	1274.5392	637.7732	1273.5551	637.2812	Q	887.2837	444.1455	870.2571	435.6322			4
13	1846.6566	923.8319	1829.6300	915.3186	1828.6460	914.8266	U	***759.2251***	380.1162	742.1986	371.6029			3
14	1903.6780	952.3426	1886.6515	943.8294	1885.6675	943.3374	G	***204.1343***	102.5708	187.1077	94.0575			2
15							K	***147.1128***	74.0600	130.0863	65.5468			1

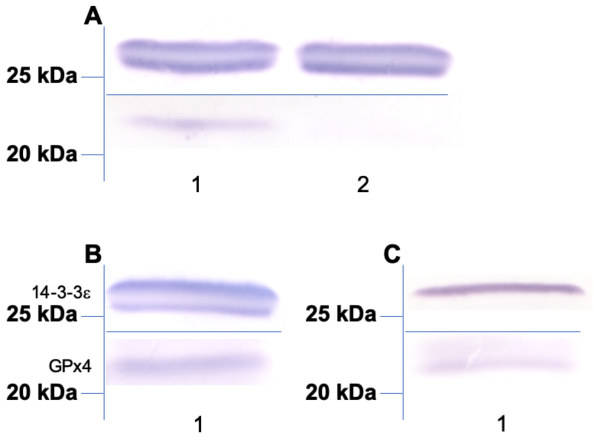
A
25 kDa
20 kDa
1
2
B
14-3-3ε
25 kDa
GPx4
20 kDa
1
C
25 kDa
20 kDa
1

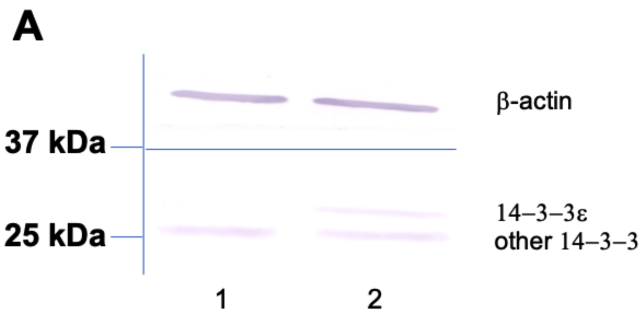
A
37 kDa
25 kDa
β-actin
14–3–3ε
other 14–3–3
1
2


C
37 kDa
25 kDa
β-actin
14–3–3ε
other 14–3–3
1
2

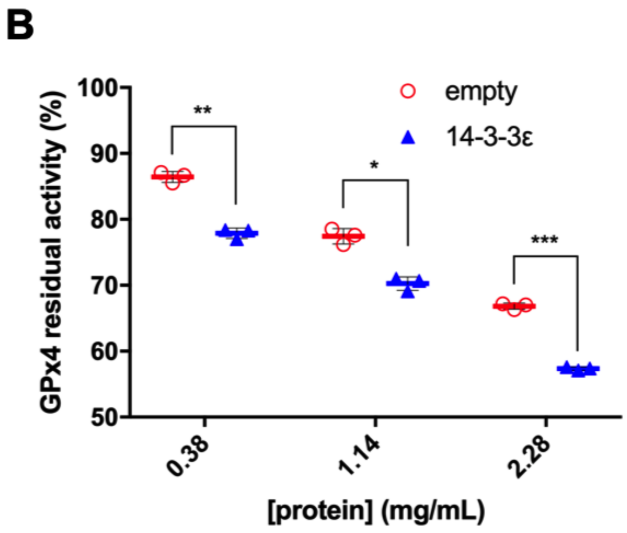
B
GPx4 residual activity (%)
100
90
80
70
60
50
empty
14-3-3ε
**
*
***
0.38
1.14
2.28
[protein] (mg/mL)

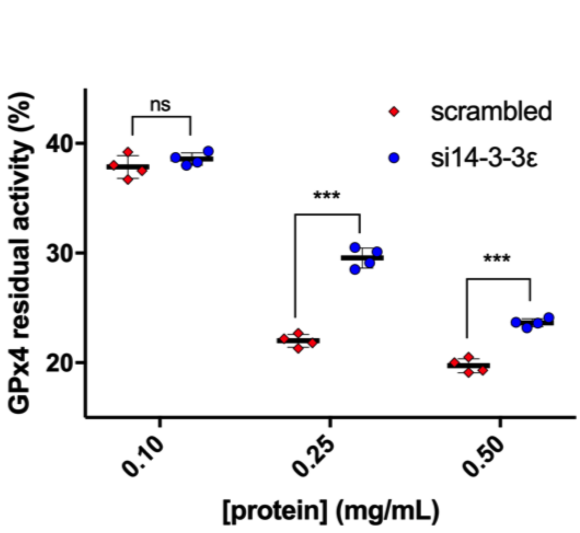
D
GPx4 residual activity (%)
40
30
20
scrambled
si14-3-3ε
ns
***
***
0.10
0.25
0.50
[protein] (mg/mL)